# Evidence of photon acceleration by laser wake fields

C. D. Murphy[a)]
*CCLRC Rutherford Appleton Laboratory, Chilton, Didcot, OX11 0QX, United Kingdom and Blackett Laboratory, Imperial College, London, SW7 2BZ, United Kingdom*

R. Trines[a)]
*CCLRC Rutherford Appleton Laboratory, Chilton, Didcot, OX11 0QX, United Kingdom*

J. Vieira
*GOLP/Centro de Física de Plasmas, Instituto Superior Técnico, Lisbon, Portugal*

A. J. W. Reitsma
*Department of Physics, University of Strathclyde, Rottenrow, Glasgow, G4 0NG, United Kingdom*

R. Bingham
*CCLRC Rutherford Appleton Laboratory, Chilton, Didcot, OX11 0QX, United Kingdom and Department of Physics, University of Strathclyde, Rottenrow, Glasgow, G4 0NG, United Kingdom*

J. L. Collier, E. J. Divall, P. S. Foster, C. J. Hooker, A. J. Langley, and P. A. Norreys
*CCLRC Rutherford Appleton Laboratory, Chilton, Didcot, OX11 0QX, United Kingdom*

R. A. Fonseca,[b)] F. Fiuza, L. O. Silva, and J. T. Mendonça
*GOLP/Centro de Física de Plasmas, Instituto Superior Técnico, Lisbon, Portugal*

W. B. Mori
*Department of Physics and Astronomy, University of California Los Angeles, Los Angeles, California 90095-1547*

J. G. Gallacher, R. Viskup, and D. A. Jaroszynski
*Department of Physics, University of Strathclyde, Rottenrow, Glasgow, G4 0NG, United Kingdom*

S. P. D. Mangles, A. G. R. Thomas, K. Krushelnick, and Z. Najmudin
*Blackett Laboratory, Imperial College, London, SW7 2BZ, United Kingdom*

(Received 1 December 2005; accepted 31 January 2006; published online 31 March 2006)

Photon acceleration is the phenomenon whereby a light wave changes color when propagating through a medium whose index of refraction changes in time. This concept can be used to describe the spectral changes experienced by electromagnetic waves when they propagate in spatially and temporally varying plasmas. In this paper the detection of a large-amplitude laser-driven wake field is reported for the first time, demonstrating photon acceleration. Several features characteristic of photon acceleration in wake fields, such as splitting of the main spectral peak and asymmetries between the blueshift and redshift for large shifts, have been observed. The experiment is modeled using both a novel photon-kinetic code and a three-dimensional particle-in-cell code. In addition to the wide-ranging applications in the field of compact particle accelerators, the concept of wave kinetics can be applied to understanding phenomena in nonlinear optics, space physics, and fusion energy research.  [DOI: 10.1063/1.2178650]

## I. INTRODUCTION

The laser wake-field accelerator is a scheme that uses the electric field of the plasma wave left in the wake of an intense ultrashort laser beam to "trap" and accelerate correctly phased charged particles to high energy.[1–8] The generation of laser wake fields has been demonstrated by acceleration of both external[9] and self-trapped electrons.[10–14] The laser's photons can also experience an upshift or a downshift in energy or frequency, i.e., photon acceleration or deceleration, as a result of the time-dependent refractive index.[15,16] The laser frequency commonly needs to be much higher than the plasma frequency, so that the space and time scales of the plasma perturbations are much larger than the photon wavelength and period. In this case, geometric optics can be used to describe the motion of the electromagnetic wave packets, as well as the influence of the plasma on this motion.[16] The action of the photons on the plasma can be described through the action of the ponderomotive force.[17]

The applications of this concept are many, not least because the accelerated waves need not necessarily be light waves. The process of wave-packet modification is known as the modulational instability, and can be used to describe a wide range of phenomena found in the interaction of light and other electromagnetic waves with plasmas. It also has many applications in nonlinear optics,[18] space physics, photon Landau damping,[19] physics of planetary atmospheres, magnetic confinement fusion,[20] and astrophysics.[21] In some

[a)]Authors C.D. Murphy and R. Trines contributed equally to this work.
[b)]Also at DCTI/Instituto Superior de Ciências do Trabalho e da Empresa, Lisboa, Portugal.

 

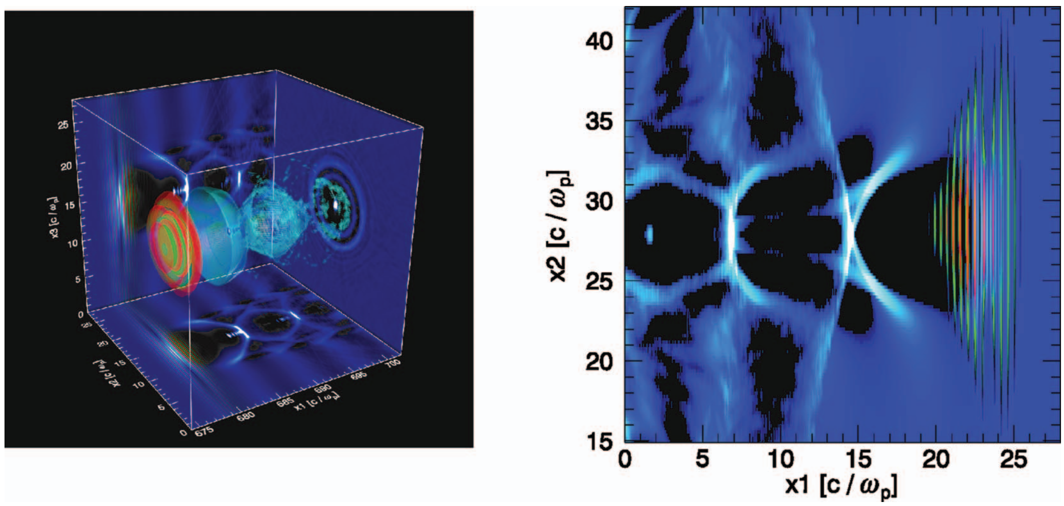


FIG. 1. (Color) Left: A typical example of a laser-driven wake field, obtained from a 3D OSIRIS simulation (see Ref. 38). The laser pulse (red/green) travels from right to left, exciting a wake field by pushing away the plasma (blue). The laser pulse has an intensity of $I\lambda^2 = 3.6\times10^{18}$ W cm$^{-2}$ $\mu$m$^2$ ($a_0=2.0$) and a wavelength of 800 nm. The plasma density is $7\times10^{18}$ cm$^{-3}$ ($\omega_0/\omega_p \sim 16$). The figure shows the laser pulse and trailing wake field after a propagation distance of 1350 $\mu$m. The projections on the bottom and side of the simulation box show the plasma density for this wake field; a small bunch of self-trapped plasma electrons can be seen near the back of each wave bucket. Such wake fields can be used to accelerate conventional particles as well as photons. Right: The wake field of a 2D OSIRIS simulation performed using the exact same parameters for laser pulse and plasma. The 2D wake field is very similar to the 2D projections of the 3D wake field pictured on the left. This proves that a 2D model is sufficiently close to a 3D one in this regime, and justifies the use of 2D OSIRIS for most of the simulations discussed in this paper.

form, the concept can be applied to virtually any system in which a broadband or turbulent spectrum of small-scale waves interacts with a coherent, large-scale structure.

It has been known for some time that light traveling away from a co-propagating region of increasing plasma density will experience a blueshift. If the increase in plasma density is caused by an ionization front associated with the traveling laser pulse, this phenomenon is called *ionization blueshift*.[22,23] In the case of an underdense plasma, the photon picture can be used to describe the increase in photon energy.[24] Photon acceleration due to relativistic ionization fronts is well documented experimentally, for microwaves,[22] as well as for light in the visible and near-infrared.[23,25,26] Alternatively, the photons of a laser pulse can also be accelerated by the wake field driven by this pulse. A typical laser-driven wake field is depicted in Fig. 1. Since the wake field comprises regions of both increasing and decreasing plasma density, photons trapped in it can be accelerated as well as decelerated, depending on their position in the wake field. Although the underlying principle is similar to photon acceleration by ionization fronts, there is no evidence in our observations that ionization fronts play a significant role; instead, all the evidence clearly points to photon acceleration by a wake field. (See also Fig. 6, where we show that laser-driven ionization processes have a negligible influence on the final spectrum.) As shown by Koga *et al.*,[27] ionization blueshift causes the laser spectrum to be blueshifted as a whole. The extent of the shift is determined by the duration of the interaction with the ionization front. On the other hand, photon acceleration by a wake field will lead to an asymmetric deformation of the spectrum while the mean frequency decreases slightly as a result of energy transfer from the pulse to the wake field.

The diagnosis of wake-field accelerators is notoriously difficult. Many of the methods suggested in the past have become infeasible at relativistic intensities due to the increasing nonlinearity of the process. One of the first methods, suggested by Hamster *et al.*, was the analysis of terahertz radiation emitted from low-amplitude plasma waves.[28] Subsequently the existence of a wake field was confirmed by observation of the relativistic electrons produced therein.[29] Some of the most ground-breaking optical probing of wake fields to date has been carried out using the technique of frequency domain interferometry (FDI).[30] This technique involves measurements of the local plasma density at a fixed phase in the wake field by observing the phase shift of a probe pulse that follows the wake-field driver at a fixed distance. This technique can only be used in low-amplitude plasma waves where the plasma gradient is small enough so as not to induce a frequency shift. In addition, the propagation distance cannot be too long, otherwise dephasing of the probe will lead to the result being averaged over the wake-field phase. Many shots are needed to obtain the profile of a single wave period, and one needs at least two pulses per shot, which must be tuned carefully in order to obtain an accurate value for the phase difference, rendering this a fairly complex method for wake-field diagnosis.

Photon acceleration, by virtue of being a single pulse and single shot, is a simpler experimental technique. A full study into the differences between frequency domain interferometry and photon acceleration was reported by Dias *et al.*;[31] we will only give a summary here. With FDI, one measures the phase difference between two pulses; this can be done accurately only if the frequency of both pulses remain more or less constant during the measurement. With photon acceleration, one measures the frequency change of the photons in the laser pulse, which is the very phenomenon that one wishes to avoid in FDI measurements. In addition, in FDI, the probe pulse propagating through the plasma must not slip with respect to the plasma wave to be diagnosed; for photon acceleration, this slippage is accounted for by default in the model. As a consequence, FDI is best suited for the diagnosis of small-amplitude plasma waves, while photon acceleration works best for large-amplitude, nonlinear plasma waves. Photon acceleration is also easier to implement experimentally: since a lot of information on the wake field can be gleaned from the details of the spectral deformations, a single shot is often sufficient to diagnose an entire wake field, and since one is studying the spectrum of the driving pulse itself, no probe pulses are needed in the measurement.

For efficient wake-field generation, the laser pulse should be shorter than the part of the plasma wave that decelerates photons (for small amplitude, this is about half the plasma wavelength: $\lambda_p = 2\pi c/\omega_p$, where $\omega_p$ denotes the plasma frequency). In this case, the entire laser pulse acts to increase the wake-field amplitude. This energy transfer to the plasma results in a redshift of the laser beam, or photon deceleration. However, if the laser pulse is made longer than optimal, the tail of the pulse will experience an upshift in energy. Upshifted photons predominantly spend much more time in the accelerating part of the wake field than downshifted photons spend in the decelerating part. This is because the maximum velocity difference between blueshifted photons and the plasma wave is $c - v_\phi$, where $v_\phi$ is the phase velocity of the plasma wave (approximately $0.995c$ in our case), so that the rate of dephasing for blue shifted photons is small. Conversely, the redshifted photons travel more slowly than the plasma wave, and therefore no such limit applies. Hence, due to this nonlinear dispersion, a characteristic asymmetry arises, with greater frequency blueshift than redshifts. By using photon acceleration, it is possible to have single-shot optical characterization of the wake field, as has been investigated theoretically.[31] This is directly analogous to diagnosis of a particle-beam-driven wake field by adding a "witness" tail to the driving beam.[32,33]

An important application of photon acceleration would be its use as a diagnostic to determine the amplitude of a laser-driven wake field. However, it is not straightforward to derive an analytical expression connecting the observed frequency shifts to the amplitude of the wake field responsible for them. One could envisage using an analytic model to obtain a quantitative measure of the plasma wave amplitude and period. The standard expression is discussed by Dias *et al.*:[31]

$$\Delta\omega \approx \frac{\omega_p^2}{2\omega_0}\frac{\delta n_{e_0}}{n_{e_0}} k_p \Delta z \cos(k_p \zeta),$$

where $\omega_0$ denotes the laser's central frequency, $\Delta\omega$ the maximum frequency shift in the laser's spectrum due to the interaction with the plasma, $\delta n_{e_0}/n_{e_0}$ the relative perturbation of the plasma density, $k_p = c/\omega_p$ the linear plasma wave number, $\Delta z$ the distance along which the laser pulse interacts with the plasma, and $\zeta$ the distance in the laser reference frame $(z - ct)$. However, in order to use this expression one must assume a linear description of the wave which is not applicable under the experimental conditions discussed in this paper. This issue remains difficult to resolve due to the strongly nonlinear character of the interaction, which all but foils any attempt to quantify the wake-field amplitude analytically.

## II. EXPERIMENTAL SETUP

Experiments were conducted using the Ti:sapphire Astra laser at the Rutherford Appleton Laboratory. The laser delivered linearly polarized pulses of wavelength $\lambda = 790$ nm [bandwidth of 20 nm full width at half-maximum (FWHM)], energy 360 mJ, and pulse duration $\tau_l = 40$ fs FWHM to target with a repetition rate of 1 Hz. The 60 mm diameter laser beam was focused onto a supersonic helium gas jet target with an $f/17$ off-axis parabolic mirror, giving a focal spot of 25 $\mu$m FWHM intensity. An equivalent plane monitor indicated that 50% of the delivered laser energy was within this focal area. The intensity on target was $I\lambda^2 = 5.7 \times 10^{17}$ W cm$^{-2}$ $\mu$m$^2$, corresponding to a peak normalized vector potential $a_0 = eE_0/(m_e\omega_0 c)$ of 0.8, where $E_0$ denotes the electric field amplitude of the laser field and $\omega_0 = 2\pi c/\lambda$ is the laser's angular frequency. The gas jet, when ionized, produced uniform plasmas for which the background density $n$ ranged from $1 \times 10^{19}$ to $3 \times 10^{19}$ cm$^{-3}$. For these densities, the characteristic period of plasma oscillation $(2\pi/\omega_p)$ ranges from $0.5\tau_l$ to $0.75\tau_l$. The supersonic gas jet ensures that the laser impinges on the gas target within one Rayleigh length of its maximum intensity. Transverse optical imaging revealed an interaction length of $\delta x \approx 650$ $\mu$m.

The light transmitted through the helium gas target was collected and collimated using a 0.44 m focal length on-axis parabolic mirror. This mirror had a clear aperture of 75 mm (approximately $f/6$) and was the limiting aperture in the collection system. The collimated light was then steered out of the vacuum chamber using flat silver-coated mirrors and focused onto the entrance slit of a 0.25 m optical spectrometer, equipped with a 150 lines/mm diffraction grating. A 16 bit CCD camera recorded the dispersed spectra on a single shot basis.

## III. EXPERIMENTAL RESULTS

The left graph in Fig. 2 shows four op tical spectra taken at different plasma densities. The dotted line indicates the central frequency of the initial laser spectrum: $\omega_0$. Several features are noticeable. Most importantly, the spectra are shifted to both lower and higher frequency with respect to $\omega_0$. However there is a clear asymmetry, with the light displaced furthest from $\omega_0$ being more intense on the "blue" side. The normalized intensity of the blueshift decreases with increasing density. The peaks on the low-energy side are caused by Raman scattering and are relatively wide. They were used to provide a relatively unambiguous measure of the plasma density $n$, since they are separated from $\omega_0$ by the plasma frequency $\omega_p = (ne^2/\epsilon_0 m_e)^{1/2}$. Many shots were used to characterize the gas jet.[11]

Previously observed laser blueshifting has been attributed solely to changes in density caused by the rapid optical field ionization.[23] However, this mechanism generates several distinct spectral characteristics that are incompatible

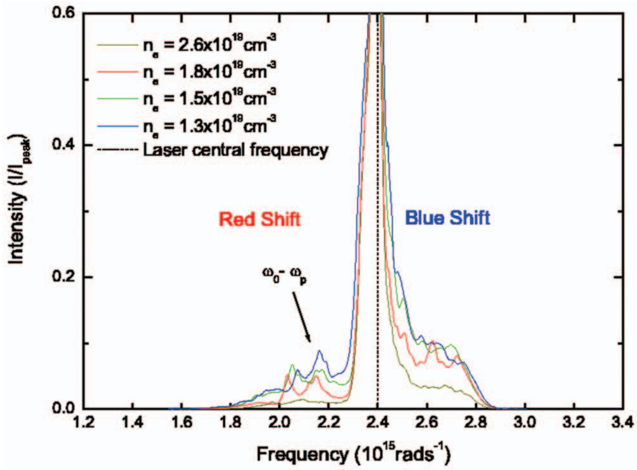


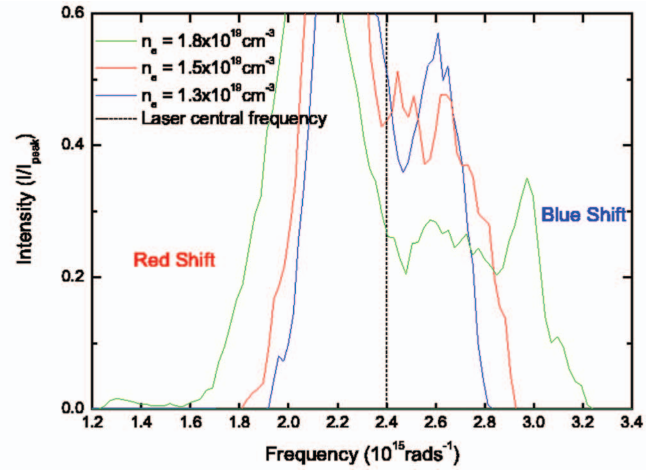


FIG. 2. (Color) (a) Optical spectra taken at different plasma densities. The blue shift is seen to increase as the density decreases. This is most noticeable when the first blue peak visible in the spectrum is considered. It has respective relative intensities of 0.20, 0.17, 0.11, and 0.06 when listed from the lowest to the highest density. The indicated peak at $\omega_0-\omega_p$ is the first Stokes peak produced by the Raman forward scattering instability. (b) Frequency spectra taken from one-dimensional photon-kinetic simulations modeled after the experiments. The behavior of the blueshifted plateau is qualitatively well reproduced by the simulations. The larger width and intensity of the simulated spectra compared to the observed ones are most likely attributed to the fact that the simulations are not three-dimensional.

with our current findings. First, ionization blueshift leads to a shift of the entire spectrum over a distance of up to 40 nm,[23,27] which is completely absent from the observations in Fig. 2. Second, the intensity of the blueshifted radiation should increase with increasing plasma density in the case of an ionization front, while in our observations it stays constant or even falls with increasing plasma density. In addition, ionization can only play a minor role in the interaction of the main pulse with the plasma because (i) at focus, almost half of the pulse's energy is at an intensity of about $10^{18}$ W/cm$^2$, while full ionization of helium requires only $10^{16}$ W/cm$^2$, so that ionization can be expected to take place only in a tiny fraction of the pulse's volume, and (ii) with the pulse focused on a narrow gas jet, there is not a significant amount of gas for the pulse to ionize before or after focus (where it has a lower intensity and ionization might occur in a significant fraction of the pulse's volume), contrary to the case of a gas-filled chamber as used by Koga *et al.*[27] Two- and three-dimensional particle-in-cell (PIC) simulations using OSIRIS that explicitly include ionization processes confirm that laser-driven ionization is not important, as discussed below.

Another phenomenon that may lead to spectral broadening in laser-plasma interaction is self-phase modulation.[34–36] Self-phase modulation is defined to be the phase and frequency shifts of light traveling through a nonlinear optical medium; it can be shown, though, to be one of many forms of photon acceleration.[16] In laser-plasma interaction, self-phase modulation manifests itself in the dependence of the photon frequency $\omega$ on the laser intensity $I \sim A^2$ (where $A$ denotes the vector potential of the laser field) through the relativistic shift in the plasma frequency $\omega_p^2$. Although self-phase modulation will certainly contribute to spectral broadening of the driving laser pulse, it is in itself a far too simplified concept to explain the modulations of the fundamental spectral peak in laser-plasma interaction using very intense pulses. It does not take into account many aspects of the interaction, such as photon acceleration/deceleration due to plasma density perturbations, phase slippage of the photons with respect to a wake field, or modulation of the pulse's intensity envelope due to photon bunching in a plasma wake field. For proper wake-field diagnosis and explanation of the observed spectral modulations, the full picture of photon acceleration is needed.

## IV. THEORY AND NUMERICAL MODELING

To model the experiment, simulations were conducted using a photon-kinetic particle code.[24,37] In this code, photons are treated as particles, while the plasma is described by cold fluid equations. These simulations give a clear qualitative picture of the dynamics of photons interacting with the plasma, allowing one to track the path of each individual photon. In addition, this method poses much lighter computational demands, while still providing qualitatively correct results, allowing one to identify the physical phenomena underlying the observed experimental results. The simulations were performed with the same parameters as the experiments. Their results are displayed in Fig. 2(b). For a few configurations, complementary simulations have been performed using the full three-dimensional (3D) particle-in-cell code OSIRIS.[38] In contrast to the photon-kinetic code, OSIRIS treats the electromagnetic fields as waves, and uses a particle model for the plasma. A comparison between the results of the photon-kinetic and the full two-dimensional (2D) and 3D PIC code runs reveals that there is excellent qualitative agreement between them, as well as between the numerical and experimental results. In Fig. 1, the results are displayed from a 3D and a 2D run having identical parameters. It can easily be seen that the wake field taken from the 2D run is very similar to the 2D projection of the 3D wake field (bottom and sides of the box containing the 3D wake field). This fully justifies the use of the wave-kinetic approach to study photon dynamics and uncover the physical mechanisms responsible for the experimentally observed laser spectra, as well as the use of the 2D simulation results in the remainder of this article.

The photon-kinetic code uses the Wigner-Moyal description for the electromagnetic fields, in which the fields are described by the photon number density: $N(t,\vec{x},\vec{k}) = \epsilon(t,\vec{x},\vec{k})/\omega(\vec{k})$, where $\epsilon(t,\vec{x},\vec{k})$ denotes the energy density of the electromagnetic field as a function of time, position, and wave vector, and $\omega(\vec{k})$ is the light's angular frequency given by the linear dispersion relation for electromagnetic wave propagation (see below). For the propagation of a laser pulse through a sufficiently underdense plasma, it can be shown that the photon number is approximately conserved locally, leading to the following (Liouville) equation for $N(t,\vec{x},\vec{k})$:[16]

$$\frac{\partial N}{\partial t} + \frac{d\vec{x}}{dt}\frac{\partial N}{\partial \vec{x}} + \frac{d\vec{k}}{dt}\frac{\partial N}{\partial \vec{k}} = 0. \tag{1}$$

The factors $d\vec{x}/dt$ and $d\vec{k}/dt$ are obtained using ray-tracing equations from geometrical optics. Using the dispersion relation for electromagnetic waves in plasma, $\omega^2 = c^2k^2 + (e^2/\epsilon_0 m_e)(n/\gamma)$, we find $d\vec{x}/dt = \partial\omega/\partial\vec{k} = c^2\vec{k}/\omega$ and $d\vec{k}/dt = -\partial\omega/\partial\vec{x} = -(1/\omega)(e^2/\epsilon_0 m_e)\partial(n/\gamma)/\partial\vec{x}$. Here, $\gamma$ denotes the relativistic Lorentz factor due to plasma electron motion. Approximating $N$ by a large number of macroparticles, where each macroparticle represents a fixed number of photons, the above equations allow one to follow the evolution of $N$ by means of a kinetic model, in which the motion of each macroparticle is governed by ray-tracing equations.

For laser-induced wake-field generation without plasma electron self-trapping, it is sufficient to use a nonlinear relativistic fluid model to describe the plasma motion. In this model, plasma perturbations are driven by the laser ponderomotive force:[17]

$$\mathbf{F_p} = -\frac{m_e c^2}{2\gamma}\nabla\left(\frac{eA}{m_e c}\right)^2, \quad A^2 = \int \frac{dk}{(2\pi)^3}\frac{N(t,\vec{x},\vec{k})}{\omega(\vec{k})}. \tag{2}$$

Assuming that the transverse electron motion is dominated by the fast quiver motion in the laser field, while the longitudinal motion is dominated by the slow wake-field oscillations, we find that $\gamma = \sqrt{1+p_z^2+\langle A^2\rangle}$, where $p_z$ denotes the average forward momentum of the oscillating plasma fluid, and $\mathbf{F_p} = -1/(2\gamma)\nabla\langle A^2\rangle$, angular brackets denoting the average over the fast laser oscillations. Note that for a laser vector potential $\mathbf{A} = \mathrm{Re}[\mathbf{A_0}\exp i(k_0x - \omega_0 t)]$, we have $\langle A^2\rangle = A_0^2$ for circular polarization, and $\langle A^2\rangle = A_0^2/2$ for linear polarization. The equation for the slow motion of the plasma electrons (cold electron fluid model, stationary ions) then reduces to $\partial\vec{p}/\partial t = -e\vec{E}_s - \mathbf{F_p}$, where $\vec{E}_s$ denotes the electrostatic field. The other two equations used to describe the plasma are Poisson's equation to obtain $\vec{E}_s$, and the continuity equation to obtain the plasma density. The ensemble of the wave-kinetic model for the laser pulse and the fluid model for the electron plasma allows us to describe the interaction between pulse and plasma in a self-consistent way.

The coupled wave-kinetic/fluid model has been implemented numerically in a 1D2V code (one spatial and two velocity dimensions), referred to as a one-dimensional (1D) code. Several configurations have also been simulated using the full 3D3V particle-in-cell code OSIRIS.[38] This code, as opposed to the photon-kinetic code, solves Maxwell's field equations on a grid, while using a particle model for the plasma. It also offers the option of having the laser field create the plasma through tunneling ionization of the background gas rather than starting with a pre-ionized plasma. This code has been used to validate the results from the photon-kinetic code. The comparison shows that the photon-kinetic code produces results that are qualitatively correct, and is very suitable for studying the general patterns of the photon dynamics and uncovering the underlying physical mechanisms. In addition, the wave-kinetic code is much less computationally demanding than the full-PIC model. For detailed quantitative predictions however, one may want to use a full-PIC code like OSIRIS, because of the more complete models it uses.

## V. SIMULATION RESULTS

Figure 3 shows the time history of the simulation phase space. Initially [Fig. 3(a)], a wake field is generated with amplitude close to its predicted value for a nonlinear plasma wave for the given initial intensity. As the pulse propagates through the plasma, photons at its front and center, that drive the plasma wave, are decelerated. This causes the pulse to be compressed in the longitudinal direction, so that the peak laser intensity increases and a nonlinear plasma wave is driven with density peaks satisfying $2 < n/n_0 < 10$. Photons at the back of the pulse do not take part in the excitation of the wake. However, being near the back of the wake wave bucket, these photons experience a time-dependent increase in the plasma density, resulting in an increase in their frequency. In the initial stage, this is seen as the spectrum splitting into two peaks around the fundamental frequency [Fig. 3(a)]. The upshift of the photons continues to a greater extent at later times, resulting in the peak on the blue side being spread into a plateau.

Figure 4 shows snapshots of the Wigner function derived from a 2D OSIRIS simulation, using the same parameters as the photon-kinetic simulation in Fig. 3. Note that the results from both codes are very similar, apart from some low-amplitude oscillations in the OSIRIS results, stemming from interference effects not yet included in the wave-kinetic approach.

For the range of densities used in our experiments, the pulse covers more than one plasma wave bucket, and as the plasma wavelength changes with the square root of the density, the number of photons eligible for acceleration will not vary too much between the lowest and highest density used. However, since the rate of evolution of the pulse increases with increased density, one expects to see an increase in the maximum photon blueshift, i.e., in the spectral width of the blueshifted shoulder. As the total number of photons in the blueshifted shoulder does not vary much, an increase in spectral width must necessary lead to a decrease in intensity of the shoulder. This is well reflected by the results from simulations [Fig. 2 (right)], where it can indeed be observed

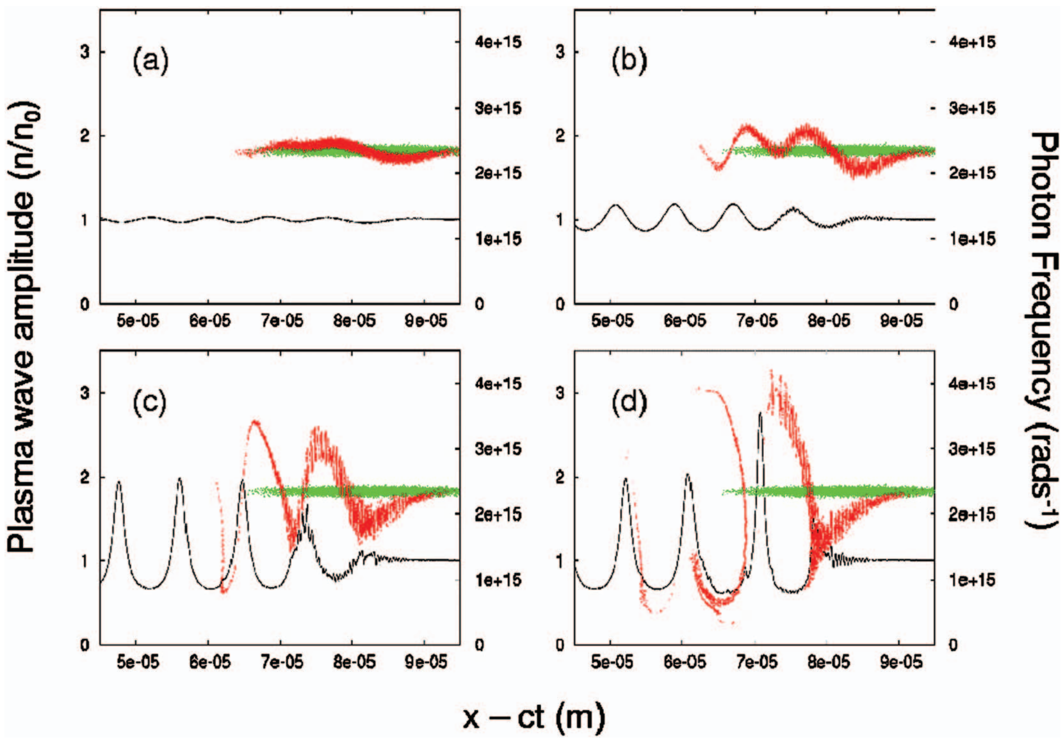


FIG. 3. (Color) Phase space plot when the laser pulse has propagated (a) 200, (b) 500, (c) 750, and (d) 1000 $\mu$m in a plasma of density $3.6\times 10^{19}$ cm$^{-3}$. The green dots denote the photon macroparticles at the beginning of the simulation. The red dots represent the photons after various propagation distances. The black line represents the generated wake-field density perturbation.

that the width of the blueshifted shoulder increases with increased density, while its intensity drops. The experimental spectra exhibit the decrease in intensity, as expected. The constant maximum blueshift in the experimental data is a phenomenon which demands further study. The mismatch between experiment and simulation is likely due to the 1D nature of the wave kinetic simulation. This means that transverse self-focusing effects, which lead to relativistic lengthening of the plasma wave, are not accurately modeled.

Another spectral characteristic, which is particularly visible for somewhat lower plasma densities, is a splitting of the fundamental peak in the laser spectrum. This is the result of the pulse interacting with a not-too-intense wake field (otherwise this spectral feature will be hidden by the imprint of other effects on the spectrum), as happens at the front and sides of the pulse. This will cause parts of the pulse to be either up-or downshifted in frequency by small amounts, comparable to the pulse's bandwidth. From the simulation results, we find that the photons are "bunching up" on either side of the central laser frequency, so that there are more photons just off than exactly at the central frequency, leading to the characteristic split peak. This is yet another piece of evidence for the existence of a wake field, as a periodic modulation of the plasma density is required to have such specific simultaneous up- and downshift. An ionization front on the other hand would yield mainly upshift, and would not lead to a visibly split central peak in the spectrum.

Experimental and simulation results are shown in Figs. 5 (left) and 5 (right), respectively, for low density ($1.3\times 10^{19}$ cm$^{-3}$) but higher laser intensity ($I\lambda^2=1.1$

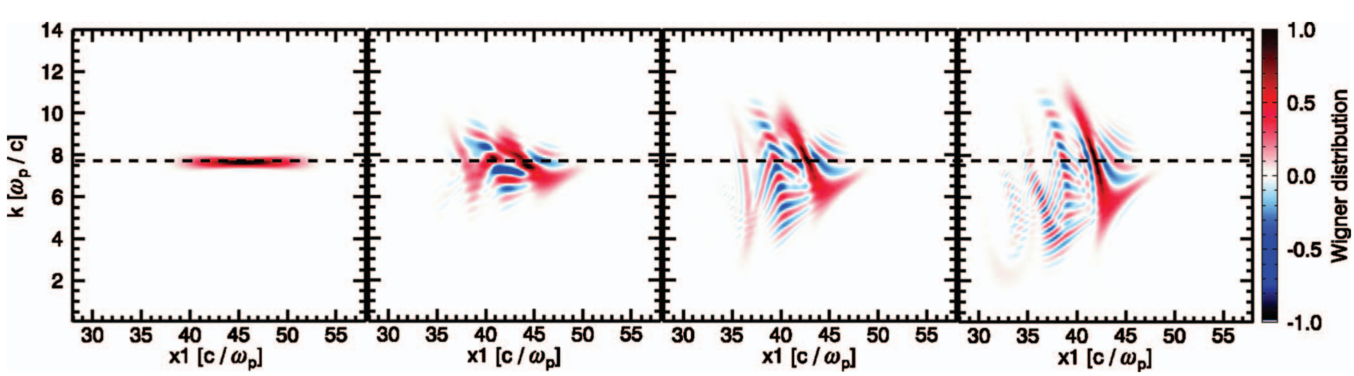


FIG. 4. (Color) Snapshots of the Wigner transform of a laser pulse propagating through a plasma of density $3\times 10^{19}$ cm$^{-3}$. The images correspond to propagation lengths of (from left to right): 0, 340, 450, and 530 $\mu$m. These snapshots were taken from a two-dimensional PIC simulation on OSIRIS. Note the similarities to the photon density plots produced by the photon-kinetic code.

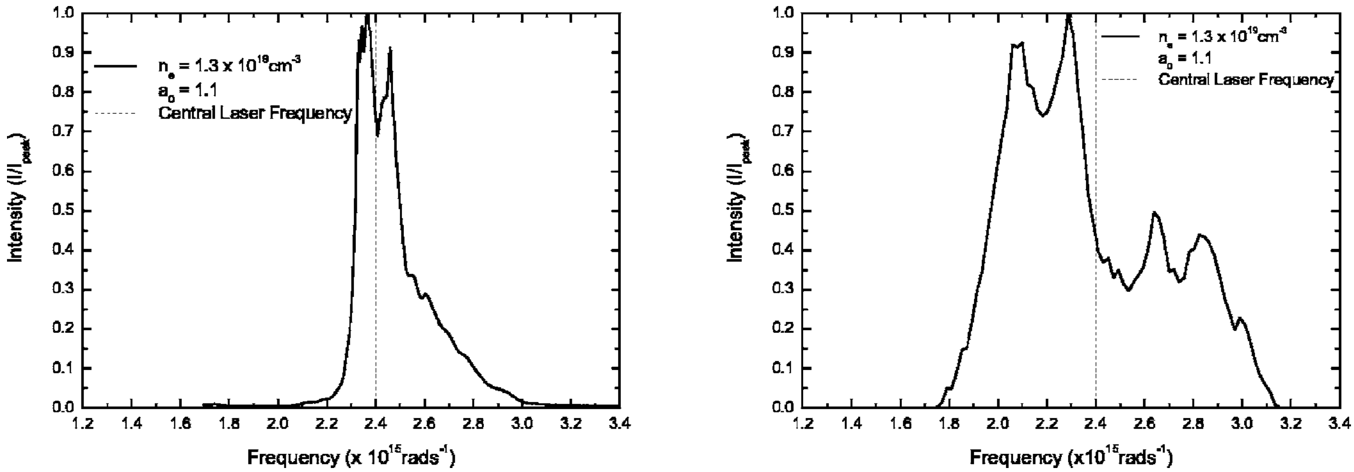


FIG. 5. Experimental (left) and photon-kinetic simulation (right) results taken at a lower plasma density ($1.3\times10^{19}$ cm$^{-3}$), but a higher laser intensity ($I\lambda^2=1.1\times10^{18}$ W cm$^{-2}$ $\mu$m$^2$, or $a_0=1.1$). The split fundamental peak is clearly visible in both cases, in addition to the "shoulder" on the blue side of the spectrum. All the features of the experimental spectrum are accurately reproduced in and explained by the simulations.

$\times10^{18}$ W cm$^{-2}$ $\mu$m$^2$, or $a_0=1.1$). Both show a frequency split in the transmitted light around $\omega_0$. In order to verify that this split does not have anything to do with the laser-driven ionization front, two additional 2D simulations have been performed using OSIRIS. In one of these a pre-ionized plasma was used, while in the other one the plasma was created by the laser pulse ionizing the background gas. Transmission spectra for both simulations are depicted in Fig. 6. Since both spectra are more or less identical, it is obvious that ionization effects do not play any role in the appearance of the split fundamental peak. This validates our earlier assertion that ionization of the background gas is almost instantaneous once the laser peak intensity is two orders of magnitude beyond the ionization threshold.

Finally, it must be emphasized that the application of the wave-kinetic approach to laser-plasma interactions has only recently emerged, and the theoretical framework has yet to be fully mature. At present, one has to rely upon numerical simulations to provide quantitative information on the wake field. In order to improve on this aspect, future work on photon acceleration will have to include an extension of the existing analytical framework to the nonlinear regime. A two-dimensional numerical model that also incorporates additional nonlinear contributions is currently under development. This will then allow us to interpret future experiments with a larger range of plasma densities and higher laser intensities.

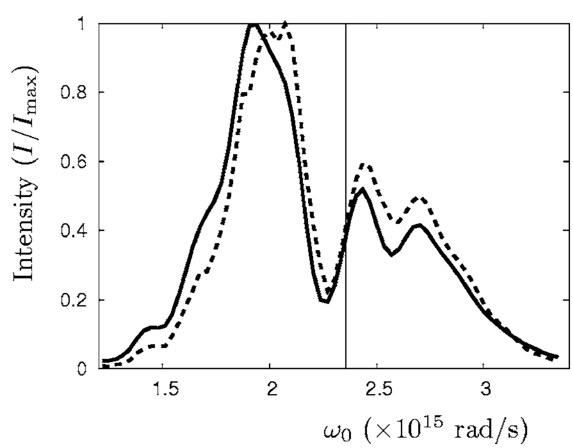


FIG. 6. Transmission spectra of intense laser pulses after interaction with a plasma, taken from two-dimensional OSIRIS simulations. The simulation parameters are: $I\lambda^2=5.7\times10^{17}$ Wcm$^{-2}$ $\mu$m$^2$ ($a_0=0.8$), $\lambda_0=800$ nm, $n_0=3.0\times10^{19}$ cm$^{-3}$ ($\omega_0/\omega_p=7.6$). The solid curve was obtained using a pre-ionized plasma, while for the dashed curve the plasma was created by the pulse itself. The fact that these curves are identical proves that laser-driven ionization effects do not influence the transmitted spectrum for the high laser intensities used in the experiments.

## VI. CONCLUSIONS

In conclusion, the observation of photon acceleration by longitudinal wake fields produced by intense laser pulses in plasmas has been reported here for the first time. A photon-kinetic treatment provides insight into the interaction and allows us to identify features arising from the photon acceleration process. Further confirmation of the results has been obtained using the 3D particle-in-cell code OSIRIS; a comparison between the results of both codes shows that the photon-kinetic results are qualitatively correct, and well suited to explain the physics underlying the experimentally obtained laser spectra. From the results of simulations both with and without laser-driven ionization effects, it has been shown that the experimental results are clearly due to photon acceleration and deceleration occurring within the laser-driven wake field. This combination of experiment and novel computational tool will prove to be a powerful diagnostic of large amplitude plasma waves of interest to plasma-based particle acceleration schemes.

## ACKNOWLEDGMENTS

The authors gratefully acknowledge the support of the staff of the Central Laser Facility, and wish to thank the OSIRIS consortium for the use of OSIRIS 2.0.

This work was supported by the Research Council's UK Basic Technology programme (Alpha-X), the UK Engineering and Physical Sciences Research Council, the CCLRC

Accelerator Science and Technology Centre, and the CCLRC Centre for Fundamental Physics. The work of J. V., R. F., F. F., and L. O. S. was partially supported by FCT (Portugal) through Grants PDCT/FP/FAT/50190/2003, and POCI/FIS/55905/2004.

[1] T. Tajima and J. M. Dawson, Phys. Rev. Lett. **43**, 267 (1979).
[2] S. Bulanov, V. I. Kirsanov, and A. S. Sakharov, JETP Lett. **50**, 198 (1989).
[3] P. Sprangle, E. Esarey, and A. Ting, Phys. Rev. A **41**, 4463 (1990).
[4] K. Nakajima, D. Fisher, T. Kawakubo *et al.*, Phys. Rev. Lett. **74**, 4428 (1995).
[5] E. Esarey, P. Sprangle, J. Krall, and A. Ting, IEEE Trans. Plasma Sci. **24**, 252 (1996).
[6] A. Ting, C. I. Moore, K. Krushelnick, C. Manka, E. Esarey, P. Sprangle, R. Hubbard, H. R. Burris, R. Fischer, and M. Baine, Phys. Plasmas **4**, 1889 (1997).
[7] A. Pukhov and J. Meyer-ter-Vehn, Appl. Phys. B: Lasers Opt. **74**, 355 (2002).
[8] C. Joshi and T. Katsouleas, Phys. Today **56**, 47 (2003).
[9] F. Amiranoff, S. Baton, D. Bernard *et al.*, Phys. Rev. Lett. **81**, 995 (1998).
[10] V. Malka, S. Fritzler, E. Lefebvre *et al.*, Science **298**, 1596 (2002).
[11] S. P. D. Mangles, C. D. Murphy, Z. Najmudin *et al.*, Nature (London) **431**, 535 (2004).
[12] C. G. R. Geddes, Cs. Toth, J. van Tilborg, E. Esarey, C. B. Schroeder, D. Bruhwiler, C. Nieter, J. Cary, and W. P. Leemans, Nature (London) **431**, 538 (2004).
[13] J. Faure, Y. Glinec, A. Pukhov, S. Kiselev, S. Gordienko, E. Lefebvre, J.-P. Rousseau, F. Burgy, and V. Malka, Nature (London) **431**, 541 (2004).
[14] T. Katsouleas, Nature (London) **431**, 515 (2004).
[15] S. C. Wilks, J. M. Dawson, W. B. Mori, T. Katsouleas, and M. E. Jones, Phys. Rev. Lett. **62**, 2600 (1989).
[16] J. T. Mendonça, *Theory of Photon Acceleration* (Institute of Physics, Bristol, 2001).
[17] L. O. Silva, R. Bingham, J. M. Dawson, and W. B. Mori, Phys. Rev. E **59**, 2273 (1999).
[18] A. Mussot, E. Lantz, H. Maillotte, T. Sylvestre, C. Finot, and S. Pitois, Opt. Express **12**, 2838 (2004).
[19] R. Bingham, J. T. Mendonça, and J. M. Dawson, Phys. Rev. Lett. **78**, 247 (1997).
[20] R. Trines, R. Bingham, L. O. Silva, J. T. Mendonça, P. K. Shukla, and W. B. Mori, Phys. Rev. Lett. **94**, 165002 (2005).
[21] C. H.-T. Wang, J. T. Mendonça, and R. Bingham, "Photon energy upshift by gravitational waves from a compact source," Nature (2006).
[22] R. L. Savage, C. Joshi, and W. B. Mori, Phys. Rev. Lett. **68**, 946 (1992).
[23] W. M. Wood, C. W. Siders, M. C. Downer, Phys. Rev. Lett. **67**, 3523 (1991).
[24] L. O. Silva and J. T. Mendonça, Opt. Commun. **196**, 285 (2001).
[25] J. M. Dias, C. Stenz, N. Lopes, X. Badiche, F. Blasco, A. Dos Santos, L. Oliveira e Silva, A. Mysyrowicz, A. Antonetti, and J. T. Mendonça, Phys. Rev. Lett. **78**, 4773 (1997).
[26] N. C. Lopes, G. Figueira, J. M. Dias, L. O. Silva, J. T. Mendonça, Ph. Balcou, G. Rey, and C. Stenz, Europhys. Lett. **66**, 371 (2004).
[27] J. K. Koga, N. Naumova, M. Kando, L. N. Tsintsadze, K. Nakajima, S. V. Bulanov, H. Dewa, H. Kotaki, and T. Tajima, Phys. Plasmas **7**, 5223 (2000).
[28] H. Hamster, A. Sullivan, S. Gordon, W. White, and R. W. Falcone, Phys. Rev. Lett. **71**, 2725 (1993).
[29] C. A. Coverdale, C. B. Darrow, C. D. Decker, W. B. Mori, K.-C. Tzeng, K. A. Marsh, C. E. Clayton, and C. Joshi, Phys. Rev. Lett. **74**, 4659 (1995); A. Modena, Z. Najmudin, A. E. Dangor *et al.*, Nature (London) **377**, 606 (1995).
[30] J. R. Marquès, J. P. Geindre, F. Amiranoff, P. Audebert, J. C. Gauthier, A. Antonetti, and G. Grillon, Phys. Rev. Lett. **76**, 3566 (1996); C. W. Siders, S. P. Le Blanc, D. Fisher, T. Tajima, M. C. Downer, A. Babine, A. Stepanov, and A. Sergeev, Phys. Rev. Lett. **76**, 3570 (1996).
[31] J. M. Dias, L. O. Silva, and J. T. Mendonça, Phys. Rev. ST Accel. Beams **1**, 031301 (1999).
[32] P. Muggli, B. E. Blue, C. E. Clayton *et al.*, Phys. Rev. Lett. **93**, 014802 (2004).
[33] B. E. Blue, C. E. Clayton, C. L. O'Connell *et al.*, Phys. Rev. Lett. **90**, 214801 (2003).
[34] Z. M. Sheng, J. X. Ma, Z. Z. Xu, and W. Yu, J. Opt. Soc. Am. B **10**, 122 (1993).
[35] S. V. Bulanov, N. M. Naumova, T. Zh. Esirkepov, and F. Pegoraro, Phys. Scr., T **63**, 258 (1996).
[36] I. Watts, M. Zepf, E. L. Clark, M. Tatarkis, K. Krushelnick, A. E. Dangor, R. Allott, R. J. Clarke, D. Neely, and P. A. Norreys, Phys. Rev. E **66**, 036409 (2002).
[37] R. Trines, L. O. Silva, R. Bingham, J. T. Mendonça, P. K. Shukla, and W. B. Mori, "A photon-in-cell code for intense, braodband radiation-plasma interactions" (to be published).
[38] R. A. Fonseca, L. O. Silva, R. G. Hemker *et al.*, Lect. Notes Comput. Sci. **2331**, 342 (2002).